Control Oriented Modeling of a Diesel Active Lean NOx Catalyst Aftertreatment System

D. Aswani, M. J. van Nieuwstadt, J. A. Cook, and J. W. Grizzle

Abstract

2004 Federal Tier II Bin 10 and California LEV I emission standards for diesel light trucks mandate tailpipe NOx levels of 0.6 g/mile. Active lean NOx catalysts(ALNC or LNC) have been proposed as a means to achieve this standard. These catalysts require the delivery of supplemental hydrocarbons in order to reduce NOx in the lean environment typical of diesel exhaust. In the system studied here, these additional hydrocarbons are injected into the exhaust system downstream of the turbocharger. Control-oriented, gray-box mathematical models are developed for diesel active lean NOx catalysts. The model is developed to represent the phenomenon relevant to NOx reduction and HC consumption, namely, the catalyst chemical reactions, HC storage in the ALNC, and heat transfer behavior on the basis of an individual exhaust element. As an illustration of how the model may be used, dynamic programming is applied to determine the optimal tradeoff of NOx conversion efficiency versus quantity of injected hydrocarbons.

I. Introduction

Lean burn engines, notably compression ignition engines or diesel engines, offer significant benefits over port fuel injected spark ignition engines in fuel economy and low speed torque performance. These benefits come at the expense of increased aftertreatment complexity. Although feedgas levels of oxides of nitrogen (NOx) are lower for lean burn engines, the conventional three way catalyst that works well for stoichiometric engines does not reduce NOx in the presence of excess oxygen. Consequently, tailpipe NOx would exceed 2004 Federal Tier II and California LEV I mandated levels without specific diesel aftertreatment. NOx aftertreatment for lean burn engines is therefore a research area of high activity. An overview of NOx aftertreatment devices is available in [10]. At the time of the writing of this article, the most practical options for diesel NOx aftertreatment are lean NOx traps [14], selective catalytic reduction or SCR, [3], and active lean NOx catalysts, [6], [8], [11]. This article deals exclusively with active lean NOx catalysts.

The Active Lean NOx Catalyst (ALNC) is typically a cordierite substrate with zeolite, platinum, and/or palladium loading. Engine fuel, i.e. hydrocarbons (HC), are injected upstream of the catalyst to provide a reducing agent for the oxides of nitrogen. It is crucial that the hydrocarbons be sufficiently atomized to provide adequate reactant surface and also prevent hydrocarbon slip to the tailpipe.

D. Aswani is with the Electrical Engineering and Computer Science Department, University of Michigan, Ann Arbor, MI 48109-2122, USA. E-mail:daswani@engin.umich.edu .

M. J. van Nieuwstadt is with Ford Motor Company, Ford Research Laboratory, Powertrain Control Systems Department, MD 2036 SRL, P.O. Box 2053, Dearborn, MI 48121-2053, USA. E-mail: mvannie1@ford.com .

J. A. Cook is with Ford Motor Company, Ford Research Laboratory, Powertrain Control Systems Department, MD 2036 SRL, P.O. Box 2053, Dearborn, MI 48121-2053, USA. E-mail: jcook2@ford.com .

J. W. Grizzle is with the Control Systems Laboratory, Electrical Engineering and Computer Science Department, University of Michigan, Ann Arbor, MI 48109-2122, USA. E-mail: grizzle@eecs.umich.edu .

The chemistry of the ALNC is complicated. Diesel fuel consists of many species of hydrocarbons that all behave differently, especially in the temperature range of interest which overlaps their evaporation and combustion temperatures. The temperature throughout the brick is far from constant and is a major factor in the reactions. The catalytic effect further adds to the complexity of the chemistry. An accurate physical description requires the inclusion of partial differential equations accounting for the spatial and temporal variation of temperature and species concentration, [7]. Unfortunately such models are typically too complex for control system analysis and design.

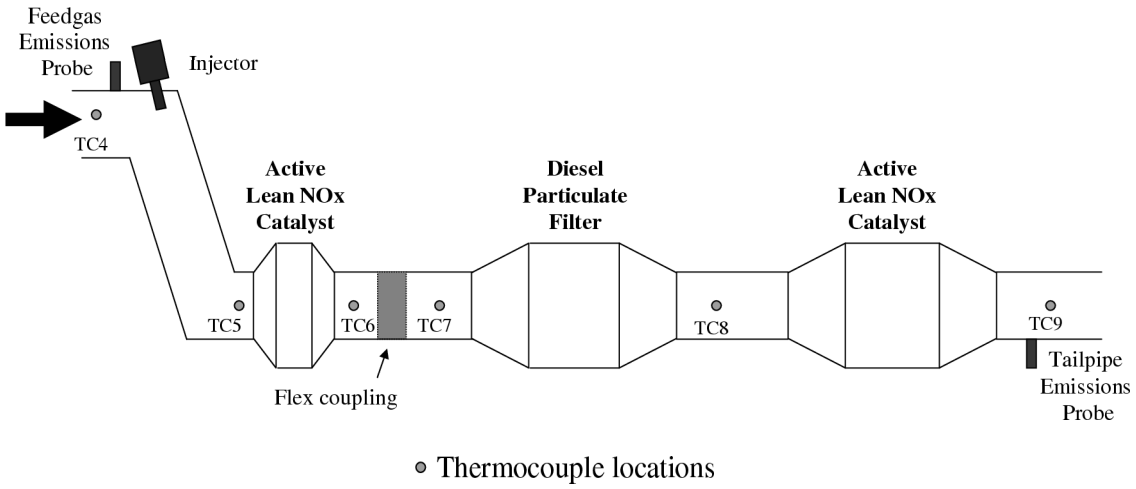

Fig. 1. Diesel exhaust aftertreatment system consisting of two active lean NOx catalysts, a diesel particulate filter and a fuel injector. Also shown are thermocouple taps, TC4 through TC9, installed for model building data collection, and emissions probes for the feedgas and tailpipe.

The present article sets out to develop a simplified model of the ALNC for control development. The overall model structure of [13] is used, with gray-box models proposed for the storage, reduction, and thermodynamic phenomena. Gray-box models are physically meaningful, simplified descriptions of the individual processes, with unknown parameters tuned via regression against experimental data. The aftertreatment system under study is depicted in Figure 1, and consists of two ALNC's and a diesel particulate filter (DPF). Ideally, the models for each component of the exhaust system could be identified individually. However, the work described in this article was conducted in parallel with engineering development, and as a result, the system modeled was restricted to the entire exhaust system of Figure 1. The model developed in Section III and IV will necessarily be a simplified representation of this aftertreatment system, though it must still capture the key phenomena associated with HC storage, NOx reduction, and the thermodynamics and heat transfer of the catalyst. To demonstrate the application of the model to control development, in Section V, dynamic programming [2] will be applied to a reduced order model of the diesel aftertreatment system. The dynamic programming algorithm will be used to determine the optimal tradeoff curve of NOx conversion efficiency versus average injected HC flow rate [5]. This

analysis will be performed on data collected over Bags 1 and 2 of the FTP 75 drive cycle. Concluding remarks are made in Section VI.

II. NOMENCLATURE

A_{cv}^{cs}	Area of generalized exhaust element void cross section (m^2)
C_p^{fg}	Exhaust gas specific heat value, 1.23 J/(mol K)
C_p^{cat}	Generalized exhaust element specific heat (J/(g K))
F	Flow rate of exhaust (mol/s)
F_a^b	Molar flow rate of X_a^b or $F \times X_a^b$ (mol/s)
F_{HC}^{inj}	Flow rate of HC injected in $C_1H_{1.8}$ (mol/s)
h_i^{conv}	Generalized exhaust element interior convective coefficient ($W/(m^2K)$)
h_o^{conv}	Generalized exhaust element exterior convective coefficient ($W/(m^2K)$)
HC	Species of HC, normalized to $C_1H_{1.8}$
κ_n	Number of HC species that oxidize for each NOx reduced in reaction "n"
$K_n(T)$	Modified Arrhenius reaction rate function of reaction "n" defined in (8)
L_{cat}	Length of generalized exhaust element (m)
m_{cat}	Mass of generalized exhaust element (g)
NOx	species of NOx, predominantly NO_2
P_{cv}^{cs}	Perimeter of generalized exhaust element void cross section (m)
P_{os}^{cs}	Perimeter of generalized exhaust element outer surface cross section (m)
P_e	Exhaust gas pressure (Pa)
Q_{LHV}	Diesel fuel lower heating value, also heat of combustion (J/mol)
R	Ideal gas constant, 8314 (L Pa)/(mol K)
T	Temperature (K)
	T_{amb}: Ambient temperature, nominally 300 K
	T^{fg}: Feedgas temperature (K)
	T_g: Exhaust gas temperature (K)
	T_p: Exhaust element temperature (K)
	(appended numbers to super/subscript indicate catalyst associaton)
V	Volume of ALNC (L)
V_{cv}	Volume of generalized exhaust element void (L)
$[\,\cdot\,]$	Concentration (mol/L)
x_{HC}^{st}	moles $C_1H_{1.8}$ stored in catalyst
	(appended numbers to super/subscript indicate catalyst associaton)
x_{HC}^{stmax}	maximum catalyst storage capacity of moles $C_1H_{1.8}$
	(appended numbers to super/subscript indicate catalyst associaton)
X_s	mole fraction of species "s"
	X_s^{fg}: mole fraction of species "s" in the feedgas
	X_s^{tp}: mole fraction of species "s" in the tailpipe
	X_s^{inlet}: mole fraction of species "s" at the inlet

(1)

III. SINGLE ALNC MODEL STRUCTURE DEVELOPMENT

The aftertreatment system under study, shown in Figure 1, consists of two ALNC's and a DPF. A model is first developed for an individual ALNC, and then these are cascaded to form a model of the

overall system. The ALNC model consists of three parts: HC storage, chemical reactions of reduction and oxidation, and heat generation and transfer. The generic model of a single ALNC will be developed in Sections III-A through III-D. An overall model of the aftertreatment system is then assembled and regressed against experimental data in Sections IV-A and IV-B, respectively. Validation against independent data is shown in Section IV-C.

A. HC Storage

The two main functional components of ALNC's are thought to be Pt sites and zeolite sites. The Pt sites help oxidize primarily CO [9]. A large fraction of HC species attach to the zeolite sites by a process described as "absorption" [9]. The HC attached in porous zeolite is believed to produce a net rich environment where NOx is reduced. However this reduction reaction also has strong temperature dependence [9]. Due to the expected strong dependence between stored HC and NOx reduction, the storage mechanism should have a significant role in the catalyst model. The HC storage mechanism is developed next.

Let x_{HC}^{st} denote the quantity of HC stored in the ALNC, in terms of the number of moles-C_1[1], and let T be the average exhaust temperature in the ALNC. It is supposed that there is an upper bound on (or maximum capacity of) the amount of HC that can be stored, denoted, x_{HC}^{stmax}. The HC storage is modeled as follows:

$$\begin{aligned}
\frac{dx_{HC}^{st}}{dt} &= K_{in}(T)\left|\frac{x_{HC}^{stmax}-x_{HC}^{st}}{x_{HC}^{stmax}}\right|^{n_1}\left(\frac{P_e}{RT}X_{HC}^{inlet}\right)^{n_3} - K_{out}(T)(x_{HC}^{st})^{n_2} - K_{3'}(T)x_{HC}^{st}\frac{P_e}{RT}X_{NOx}^{inlet} \\
F_{NOx}^{cheminlet} &= X_{NOx}^{inlet}\left(F - K_3(T)x_{HC}^{st}\frac{P_e}{RT}\right) \qquad (2) \\
F_{HC}^{cheminlet} &= FX_{HC}^{inlet} - \frac{dx_{HC}^{st}}{dt}
\end{aligned}$$

The HC storage model describes storage increase as being dependent on empty storage sites available (3) (where x_{HC}^{st} denotes stored HC) and inlet HC concentration (4). Storage loss is modeled as the combination of released HC (5), and a term including reaction of stored HC with NOx (6). Due to the consumption of NOx and loss/release of HC, flows of those species are modified for the cascaded chemical model to the terms $F_{NOx}^{cheminlet}$ and $F_{HC}^{cheminlet}$ respectively.

[1]moles-C_1 denotes the carbon atom count for hydrocarbons, having an empirical molecular formula $C_1H_{1.8}$.

Empty storage sites available: $$\left|\frac{x_{HC}^{stmax}-x_{HC}^{st}}{x_{HC}^{stmax}}\right|^{n_1} \tag{3}$$

Inlet HC concentration: $$\left(\frac{P_e}{RT}X_{HC}^{inlet}\right)^{n_3} \tag{4}$$

Rate of HC release: $$K_{out}(T)(x_{HC}^{st})^{n_2} \tag{5}$$

Reacted stored HC with NOx: $$K_{3'}(T)x_{HC}^{st}\frac{P_e}{RT}X_{NOx}^{inlet} \tag{6}$$

All $K_n(T)$ are Arrhenius reaction rates, scaled by residence time,

$$K_n(T) = k_n\ exp\left(-\frac{E_n}{T}\right)\frac{P_e}{RT}\sqrt{\frac{V}{F}}, \tag{7}$$

where k_n and E_n are constants to be determined from data. However, when fitting to data, it was found that the NOx reduction reactions were very insensitive to temperature below a certain threshold and were more appropriately modeled as

$$K_n(T) = \begin{cases} k_n\ exp\left(-\frac{E_n}{T}\right)\frac{P_e}{RT}\sqrt{\frac{V}{F}} & ,\ T > T_{cut} \\ k_n\ exp\left(-\frac{E_n}{T}\right)\frac{P_e}{RT}\sqrt{\frac{V}{F}}\ exp\left(-\frac{T-T_{cut}}{30}\right) & ,\ \text{otherwise} \end{cases} \tag{8}$$

where k_n, E_n, and T_{cut} are constants to be determined from data. Also, $K_{n'}(T) = \kappa_n K_n(T)$, for which κ_n is some constant that reflects the number of HC species that oxidize for each NOx reduced in reaction "n".

B. Chemical Reactions

The chemical reaction model treats the ALNC as a lumped, uniformly mixed, chemical reactor. It is assumed that pressure is constant in the ALNC at a value P_e and that oxygen is sufficiently plentiful that the combustion of HC does not significantly alter the concentration of O_2 from its level in the feedgas. Finally, all oxides of nitrogen are lumped as a single species, NOx (NO_2 by weight), and all hydrocarbons are lumped into a single species denoted HC ($CH_{1.8}$ by weight). The model is

$$\frac{d}{dt}[NOx] = -K_1(T)[HC][NOx] + \frac{F_{NOx}^{cheminlet}}{V} - \frac{FRT}{P_e}[NOx] \tag{9}$$

$$\frac{d}{dt}[HC] = -K_{1'}(T)[HC][NOx] - K_2(T)[HC]\sqrt{[O_2]} + \frac{F_{HC}^{cheminlet}}{V} - \frac{FRT}{P_e}[HC] \tag{10}$$

where $K_n(T)$ are reaction rates modeled with the same structure of (8). Change in $[NOx]$ is defined as the cumulative effect of loss via reduction by HC (11), flow of NOx in (12), and flow of NOx out (13). Change in $[HC]$ is defined as the cumulative effect of loss via oxidation by NOx (14), loss via oxidation

by O_2 (15), flow of HC in (16), and flow of HC out (17).

$$\textbf{NOx reduction by HC:} \quad K_1(T)[HC][NOx] \tag{11}$$

$$\textbf{Flow of NOx in:} \quad \frac{F_{NOx}^{cheminlet}}{V} \tag{12}$$

$$\textbf{Flow of NOx out:} \quad \frac{FRT}{P_e}[NOx] \tag{13}$$

$$\textbf{HC oxidation by NOx:} \quad K_{1'}(T)[HC][NOx] \tag{14}$$

$$\textbf{HC oxidation by } \mathbf{O_2}\textbf{:} \quad K_2(T)[HC]\sqrt{[O_2]} \tag{15}$$

$$\textbf{Flow of HC in:} \quad \frac{F_{HC}^{cheminlet}}{V} \tag{16}$$

$$\textbf{Flow of HC out:} \quad \frac{FRT}{P_e}[HC] \tag{17}$$

Three quantities are computed as outputs of the model, namely, the mole fractions of NOx and HC exiting the catalyst, X_{NOx}^{outlet} and X_{HC}^{outlet} respectively, and the rate of HC oxidized in the catalyst, F_{HC}^{burned}, (mol/s). The latter is needed in the thermodynamic model; note that the heat change associated with the oxidation of HC (a single $C_1H_{1.8}$) by NOx (also reduction of NOx by HC) is assumed to be the same as that resulting from oxidation of HC (a single $C_1H_{1.8}$) by O_2. Since most HC is oxidized by O_2, errors in the overall heat change estimate resulting from this assumption are small. These outputs are easily computed as follows:

$$\begin{aligned} X_{NOx}^{outlet} &= \frac{RT}{P_e}[NOx] \\ X_{HC}^{outlet} &= \frac{RT}{P_e}[HC] \\ F_{HC}^{burned} &= F_{HC}^{cheminlet} - \frac{FRT}{P_e}[HC] \end{aligned} \tag{18}$$

C. Thermodynamics

The primary goal of the thermodynamic model is to predict the temperatures needed for the chemical reaction and storage models, namely the exhaust gas temperature as it passes through the ALNC's. This requires that the temperature from the feedgas measurement be propagated to the front of the first ALNC, and that the temperatures between ALNC's be propagated from one to another. Hence, some spatial information is required as well. To accomplish this, the exhaust system is divided or lumped into eight distinct sections. In doing so, the inlet and exit cones of the ALNC's are treated as portions of the connecting pipes and were lumped with the pipes and not with the catalysts. The model treats the heat transfer of each generalized exhaust element as two processes - the convection between the pipe and ambient and the convection between the pipe and interior exhaust gases. These two thermodynamic processes approximate the entire thermodynamic behavior such that spatial temperature variations and

temperature dynamics are decoupled. The heat balance between exhaust gas and the pipe interior surface captures spatial temperature variations - Process A. The heat balance of the exhaust element body between ambient and interior gases captures the dynamics due to thermal mass of the exhaust element - Process B.

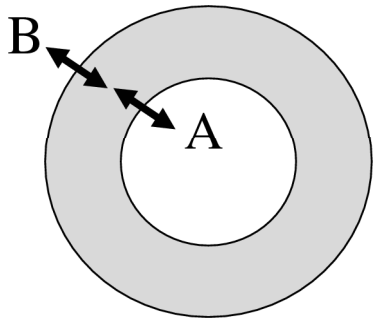

Fig. 2. Pipe and catalyst thermodynamic processes relative to cross section.

The exhaust system of Figure 1 is modeled as a series of the following components:

Section 1: the section of pipe from the feedgas temperature measurement, TC4, to the front of ALNC-1;

Section 2: the catalytic brick of ALNC-1;

Section 3: the section of pipe from the rear of ALNC-1 to the front of the DPF;

Section 4: the brick of the DPF;

Section 5: the section of pipe from the rear of the DPF to the mid-point thermocouple in the pipe, TC8;

Section 6: the section of pipe from the mid-point thermocouple in the pipe, TC8, to the front of ALNC-2;

Section 7: the catalytic brick of ALNC-2;

Section 8: the section of pipe from the rear of ALNC-2 to the tailpipe exit.

The key difference between a section of pipe, the DPF, or an ALNC is the exothermic oxidation reaction of HC which takes place in the ALNC that does not take place in a pipe or the DPF. In all other regards, the same modeling assumptions will be used in each section of the thermodynamic model.

1) Process A: Exhaust Element to Element Interior Heat Transfer Model: Let x (m) be a position measured from the left end of the exhaust element. By conservation of energy, from Figure 3,

$$\dot{Q}_{cond}(x) + \dot{Q}_{flow}(x) + \dot{Q}_{gen}(x) = \dot{Q}_{cond}(x+dx) + \dot{Q}_{flow}(x+dx) + \dot{Q}_{conv}(x) \tag{19}$$

Applying the following assumptions to the small differential length cavity depicted in Figure 3,

1) constant pressure;
2) C_p^{fg} is constant with temperature and air to fuel ratio;
3) molar flow in equals the molar flow out;

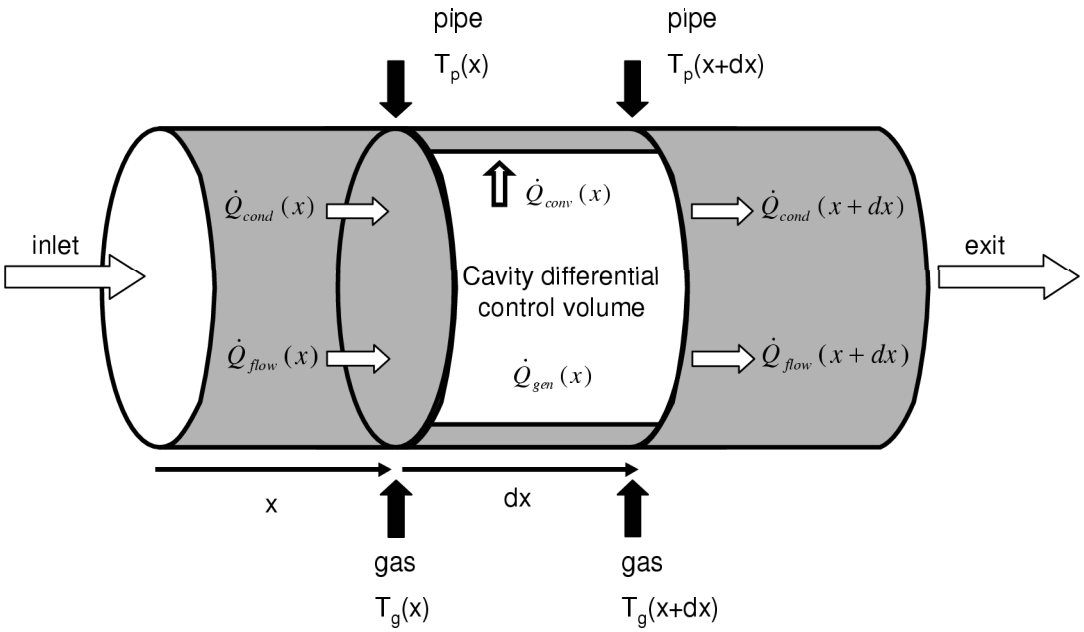

Fig. 3. General constant-pressure exhaust element differential length cavity model.

4) exhaust element cross sectional temperature is constant;
5) heat generation is dominated by HC oxidation;
6) chemical reaction is uniform throughout a catalyst brick[2];
7) conduction along the cylinder is negligible;

results in

$$\begin{aligned}
\dot{Q}_{conv}(x) &= (T_g(x) - T_p(x))\, h^i_{conv} P^{cs}_{cv} dx, \\
\dot{Q}_{gen}(x) &= \dot{q} A^{cs}_{cv} dx, \\
\dot{Q}_{cond}(x) &= \dot{Q}_{cond}(x+dx) = 0, \\
\dot{Q}_{flow}(x) &= F C^{fg}_p T_g(x), \\
\dot{Q}_{flow}(x+dx) &= F C^{fg}_p T_g(x+dx),
\end{aligned} \tag{20}$$

where, $\dot{q} = \frac{F^{burned}_{HC}}{V_{cv}} Q_{LHV}$, the rate of heat generation per unit volume, is computed by determining the amount of HC burned in the catalyst per unit time and per unit volume on the basis of the chemical model of Section III-B, V_{cv} = total volume of catalyst void, P^{cs}_{cv} = perimeter of catalyst void cross section, A^{cs}_{cv} = area of catalyst void cross section, h^i_{conv} = catalyst interior convective coefficient, C^{fg}_p = molar specific heat of exhaust gas, and Q_{LHV} = molar heat of combustion of $C_1H_{1.8}$ species. Performing an energy balance and using Taylor's Theorem to approximate $T_g(x+dx)$ by $T_g(x) + \frac{\partial T_g}{\partial x}(x)dx$ results in

$$\dot{q} A^{cs}_{cv} = F C^{fg}_p \frac{\partial T_g(x)}{\partial x} + (T_g(x) - T_p(x))\, h^i_{conv} P^{cs}_{cv} \tag{21}$$

[2]In reality, the majority of chemical reaction takes place in the early portion of the catalyst.

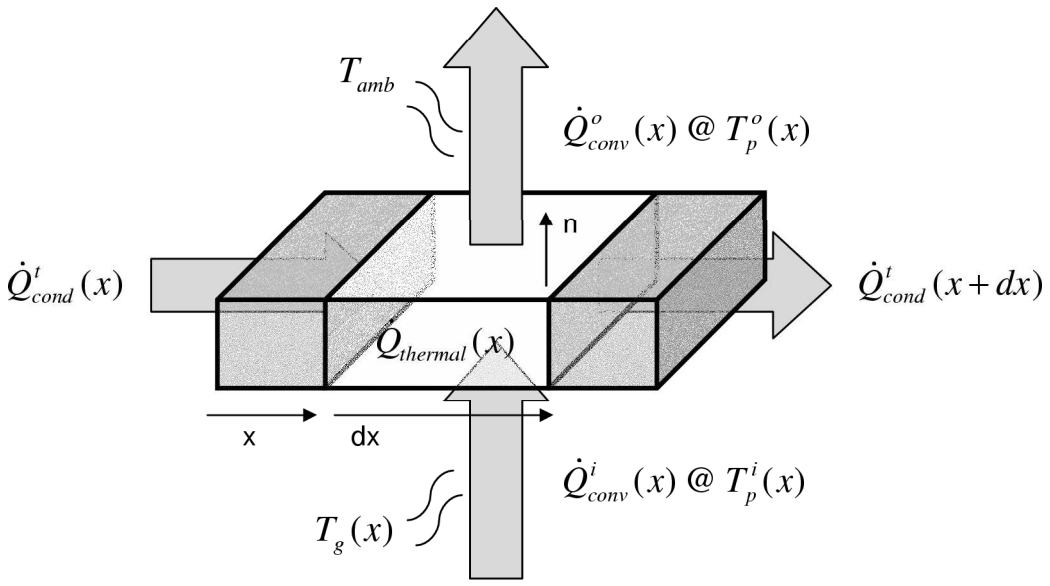

Fig. 4. General exhaust element brick/body model.

2) Process B: Exhaust Element to Ambient Heat Transfer Model: It is assumed that each exhaust element has a uniform temperature due to the high heat conductivity of the individual metal body.[3] This means that radial and transverse temperature gradients are very small, or $T^i_p = T^o_p$ and $T_p(x) = T_p(x+dx)$ (see Figure 4). It is also assumed that the exhaust element's transverse heat conduction to neighboring exhaust elements is negligible compared to its radial heat loss to ambient. T_{amb} is the ambient temperature, assumed to be 300 K. Given these additional assumptions,

$$\begin{array}{ll} \dot{Q}^o_{conv}(x) & = (T_p - T_{amb})\, h^o_{conv} P^{cs}_{os} dx, \\ \dot{Q}^i_{conv}(x) & = (T_g(x,t) - T_p)\, h^i_{conv} P^{cs}_{cv} dx, \\ \dot{Q}_{thermal}(x) & = \frac{m_{cat} C^{cat}_p}{L_{cat}} dx \frac{\partial T_p}{\partial t}, \\ \dot{Q}^t_{cond}(x) & = \dot{Q}^t_{cond}(x+dx) = 0. \end{array} \tag{22}$$

By conservation of energy,

$$\dot{Q}^t_{cond}(x) + \dot{Q}^i_{conv}(x) = \dot{Q}^t_{cond}(x+dx) + \dot{Q}^o_{conv}(x) + \dot{Q}_{thermal}(x). \tag{23}$$

After substitution,

$$(T_g(x,t) - T_p)\, h^i_{conv} P^{cs}_{cv} = (T_p - T_{amb})\, h^o_{conv} P^{cs}_{os} + \frac{m_{cat} C^{cat}_p}{L_{cat}} \frac{\partial T_p}{\partial t}, \tag{24}$$

where the new parameters P^{cs}_{os} - perimeter of outer surface cross section and h^o_{conv} - catalyst exterior convective coefficient are introduced. In explicit form this is

$$\frac{\partial T_p}{\partial t} = \frac{L_{cat}}{m_{cat} C^{cat}_p} \left[(T_g(x,t) - T_p)\, h^i_{conv} P^{cs}_{cv} - (T_p - T_{amb})\, h^o_{conv} P^{cs}_{os} \right] \tag{25}$$

[3]This is a particularly strong assumption for large metal mass elements such as the ALNC and DPF.

3) Combination of Processes A and B: The assumption that T_p is independent of position throughout each exhaust element, while allowing discontinuities in T_p at transitions from one element to another, reduces (21) to a homogeneous PDE that can be solved to yield

$$T_g(x) = \left(T_p + \frac{\dot{q}A_{cv}^{cs}}{h_{conv}^{i}P_{cv}^{cs}}\right) + \left(T_g(0) - T_p - \frac{\dot{q}A_{cv}^{cs}}{h_{conv}^{i}P_{cv}^{cs}}\right) exp\left(\frac{-h_{conv}^{i}P_{cv}^{cs}}{FC_p^{fg}}x\right). \tag{26}$$

Since T_p, $\dot{q}$, and F act as forcing terms to (26), $T_g(x)$ is in fact $T_g(x,t)$. (26) shows that $T_g(x,t)$ is also a function of T_p where T_p has a time varying coefficient. Therefore (24) becomes a time-varying PDE.

D. Single ALNC Model

The subsystem models for HC storage, NOx reduction, HC oxidation and heat transfer developed in Sections III-A through Sections III-C must be assembled into an overall lumped model of a single ALNC. This becomes

$$\begin{aligned}
T &= \frac{T_g(0,t) + T_g(L,t)}{2} && (27)\\
\frac{dx_{HC}^{st}}{dt} &= K_{in}(T)\left|\frac{x_{HC}^{stmax} - x_{HC}^{st}}{x_{HC}^{stmax}}\right|^{n_1}\left(\frac{P_e}{RT}X_{HC}^{inlet}\right)^{n_3} \\
&\quad -K_{out}(T)(x_{HC}^{st})^{n_2} - K_{3'}(T)x_{HC}^{st}\frac{P_e}{RT}X_{NOx}^{inlet} && (28)\\
F_{NOx}^{cheminlet} &= X_{NOx}^{inlet}\left(F - K_3(T)x_{HC}^{st}\frac{P_e}{RT}\right) && (29)\\
F_{HC}^{cheminlet} &= FX_{HC}^{inlet} - \frac{dx_{HC}^{st}}{dt} && (30)\\
\frac{dx_{NOx}}{dt} &= -K_1(T)x_{HC}x_{NOx} + \frac{F_{NOx}^{cheminlet}}{V} - \frac{FRT}{P_e}x_{NOx} && (31)\\
\frac{dx_{HC}}{dt} &= -K_{1'}(T)x_{HC}x_{NOx} - K_2(T)x_{HC}\sqrt{[O_2]} + \frac{F_{HC}^{cheminlet}}{V} - \frac{FRT}{P_e}x_{HC} && (32)\\
F_{HC}^{burned} &= F_{HC}^{cheminlet} - \frac{FRT}{P_e}x_{HC} && (33)\\
\dot{q} &= \frac{F_{HC}^{burned}}{V}Q_{LHV} && (34)\\
\frac{\partial T_p}{\partial t} &= \frac{L_{cat}}{m_{cat}C_p^{cat}}\left[\left(T_g(x,t) - T_p\right)h_{conv}^{i}P_{cv}^{cs} - \left(T_p - T_{amb}\right)h_{conv}^{o}P_{os}^{cs}\right] && (35)\\
T_g(x,t) &= \left(T_p + \frac{\dot{q}A_{cv}^{cs}}{h_{conv}^{i}P_{cv}^{cs}}\right) + \left(T_g(0,t) - T_p - \frac{\dot{q}A_{cv}^{cs}}{h_{conv}^{i}P_{cv}^{cs}}\right) exp\left(\frac{-h_{conv}^{i}P_{cv}^{cs}}{FC_p^{fg}}x\right) && (36)\\
X_{NOx}^{outlet} &= \frac{RT}{P_e}x_{NOx} && (37)\\
X_{HC}^{outlet} &= \frac{RT}{P_e}x_{HC}. && (38)
\end{aligned}$$

In the above, L is the length of the catalyst, $x_{NOx} = [NOx]$, and $x_{HC} = [HC]$. $K_n(T)$ are modified Arrhenius form terms as seen in (8) and $K_{n'}(T) = \kappa_n K_n(T)$, for which κ_n is some constant that reflects

the number of HC species that oxidize for each NOx reduced in reaction "n". As shown in (27), all T for storage and chemical reaction computation are taken as the average of $T_g(0,t)$ before the exhaust element and $T_g(L,t)$ after the exhaust element.

IV. Overall Exhaust System Model - Construction, Regression, and Validation

A. Overall Exhaust System Model Construction

The overall model of the exhaust system is obtained by cascading the individual models developed previously. The inputs to Sections 2 through 8 of the model are determined from the conditions at the exit of the respective previous sections. In the overall system, exhaust transport delays need not be considered since they are a fraction of a second and emissions data sampling was only available every one second.[4]

Section 1: It is assumed that no chemical reactions take place [5]. The mole fraction of HC in the exhaust gas is given by the sum of the HC in the feedgas plus the injected HC. Thus,

$$X_{HC}^{inlet} = X_{HC}^{fg} + \frac{F_{HC}^{inj}}{F}. \tag{39}$$

The thermal relationship resulting from the combination of (25) and (26) with $\dot{q} = 0$ is used to determine the temperature at the end of this section from the measurement of the feedgas temperature at the beginning of the section.

Section 2: The model (27)-(38) is used.

Section 3: It is assumed that no chemical reactions take place. The thermal relationship resulting from the combination of (25) and (26) with $\dot{q} = 0$ is used to determine the temperature at the end of this section from the exhaust gas temperature at the end of the previous section.

Section 4: Same as Section 3. (It is assumed that no chemical reactions take place when the DPF is not being forced to purge particulates.)

Section 5: Same as Section 3.

Section 6: Same as Section 3.

Section 7: The model (27)-(38) is used.

Section 8: Same as Section 3.

The required inputs to the model are feedgas flow rate F; species concentrations X_{NOx}^{fg}, X_{HC}^{fg}, and X_{O_2}; temperature T^{fg}; pressure P_e; and injected hydrocarbon flow rate F_{HC}^{inj}. The latter quantity is viewed as the control actuator while the first six quantities determine the properties of the feedgas entering the exhaust aftertreatment system. The outputs of the model are arbitrarily selected to be the tailpipe mole fraction concentrations of NOx and HC, X_{NOx}^{tp} and X_{HC}^{tp} respectively, as determined at the outlet of the

[4]Comparison of feedgas and tailpipe emissions probe data confirms this.

[5]Inspection of the thermocouple traces confirms that very little if any of the injected hydrocarbons burns before entering the catalyst.

second catalyst; T_p, the body temperature states of each exhaust element section; and T_g, the exhaust gas temperature between exhaust element sections. This model structure is similar to that proposed in [13].

B. Model Regression Against Data

The goal of this section is to estimate the unknown coefficients in the model of Section IV-A by regression against measured data. While it would be advantageous to isolate each piece of the model and design specific test sequences to identify the coefficients appearing in each section of the model, this was not feasible with the system configuration and test facilities. The available measurements were the concentrations of NOx and HC in the feedgas and tailpipe, the concentration of O_2 in the feedgas, the volume flow rate of the feedgas, and the temperature at the thermocouple locations indicated in Figure 1. For the purpose of fitting and validating the model, the temperatures at thermocouple locations TC5, TC6, TC7, TC8, and TC9 shown in Figure 1 were all used. The exhaust pressure was taken to be a constant and estimated to be $P_e = 130$ kPa[6].

1) Model Discretization: The sample rate of the measurement sets was 1 Hz. The exhaust system model was therefore discretized to a set of difference equations at a sample rate of 1 Hz in order to be compatible with data. The time scales of the chemical reactions represented by (31) and (32) were estimated to be too fast to be discretized with this sample rate, and thus these two equations were replaced with their steady state values. For each of the ALNC models, the left-hand sides of (31) and (32) were set equal to zero to yield the algebraic equations of steady state values [7] of x_{NOx} and x_{HC}, resulting in

$$x_{NOx}^{ss} = f_{NOx}(F, F_{HC}^{cheminlet}, F_{NOx}^{cheminlet}, X_{O_2}, P_e, T, R, V, k_1, k_{1'}, E_1, k_2, E_2) \quad (40)$$

$$x_{HC}^{ss} = f_{HC}(F, F_{HC}^{cheminlet}, F_{NOx}^{cheminlet}, X_{O_2}, P_e, T, R, V, k_1, k_{1'}, E_1, k_2, E_2). \quad (41)$$

The steady state values were then used in place of x_{NOx} and x_{HC} in (27)-(38). Simulation and comparison with real data shows that the time dependence in (24), mentioned in Section III-C.3, is slow enough that use of time-varying coefficients for the discretized time-invariant solution accurately approximates the system.

The overall model has a total of eighteen state variables: 2 stored HC states - one in each of the catalyst models, 8 thermal states - one for each exhaust system section, and 8 implicit states - one for each exhaust section. The implicit states are a computational detail for simple causal implementation because of the definition in (27). (27) reveals the need in the chemical model for values generated by the subsequently

[6]In reality, exhaust pressure P_e is a function of position x and flow rate F. However, the variations in P_e are small enough that assumption of $P_e = 130$ kPa (constant) does not affect the model's prediction capability.

[7]The equations were solved using the symbolic toolbox in MATLAB®. (MATLAB is a registered trademark of The MathWorks, Inc.,Natick, MA.)

applied thermal model. As a result, $T_g(L,t)$ values are approximated by a delayed $T_g(L,t)$ from a prior application of the full model. So in discrete form the additional "implicit" state appears in the form of $T_g(L,k-1)$ for each exhaust element, where k is the time index.

TABLE I

GEOMETRIC COEFFICIENTS ESTIMATED BY DIRECT MEASUREMENT OR ACCORDING TO SPECIFICATIONS.

	Exhaust Section						
	1	2	3	4	5 & 6	7	8
Length (m)	0.591	0.081	0.483	0.254	0.229	0.248	0.457
Radius (m)	0.038	0.076	0.057	0.114	0.057	0.079	0.044
Volume (L)	*	1.48	*	*	*	6.97	*
P_{os}^{cs} (m)	0.239	0.479	0.359	0.718	0.359	0.499	0.279
P_{cv}^{cs} (m)	0.239	41.8	0.359	16.9	0.359	45.4	0.279
A_{cv}^{cs} $(\times 10^{-3} m^2)$	4.56	9.68	10.3	17.5	10.3	10.5	6.21
Heat Capacity, mC_p (J/K)	301	741	369	6359	175	2451	272
x_{HC}^{stmax} (mol $C_1H_{1.8}$)	*	0.217	*	*	*	1.029	*

2) Coefficients: Known Versus to be Determined: A number of the parameters appearing in the overall exhaust system model were available by specification or could be determined by direct measurements. These are summarized in Table I. Catalyst heat capacities are by specification and pipe heat capacities are estimated by pipe wall thickness. x_{HC}^{stmax} is computed from the catalyst specification of 35 mg HC/cu.in. saturation limit. The specific heat of the exhaust gas was estimated from Table A.6 of [12] to be $C_p^{fg} = 1.23$, (J/(mol K)) and was used at this value in the model. Q_{LHV} is computed to be approximately $6.17 \times 10^5 J/mol$ $C_1H_{1.8}$ from the heat release of diesel fuel (heat of vaporization is negligible relative to this value) [4]. The T_{cut} parameter was chosen to be 200 °C. Conversion performance vastly decreased for low exhaust temperatures, which was suspected to occur due to poor vaporization of injected diesel fuel. The value 200 °C was chosen partly as a safety precaution to avoid testing that could risk HC slip through the exhaust system. The following parameters are to be estimated from data:

Storage Model: k_{in}, E_{in}, k_{out}, E_{out}, n_1, n_2, n_3, k_3, $k_{3'}$, and E_3, with the same values used in all three catalysts.

Chemical Model: k_1, $k_{1'}$, E_1, k_2, and E_2, with the same values used in all three catalysts.

Thermal Model: h_{conv}^i and h_{conv}^o for each section of the exhaust aftertreatment system. The arbitrary assumption of 16 cpsi (cells per square inch) in the DPF and catalyst is used to compute P_{cv}^{cs} through physical parameters as shown in Table I, which affects h_{conv}^i by a constant multiplier. Since cpsi is embedded as a factor into h_{conv}^i, which is an optimized parameter, choice of cpsi is irrelevant and can be arbitrary. Having the assumed cpsi closer to the actual cpsi will only keep h_{conv}^i at more

consistent values relative to the inner convective coefficients of the other elements. [8]

This results in a total of twenty-nine parameters to extract from data. (Sections 5 and 6 of the exhaust aftertreatment system are the same pipe divided into two equal sections and hence share the same coefficients.) Equality of the storage and reaction rate coefficients across both catalysts is forced once again to keep coefficient counts low.

3) Coefficient Estimation: The exhaust aftertreatment model was regressed against measured data so as to minimize a cost determined on the basis of tailpipe flows of NOx and HC as well as the exhaust system thermocouples TC5, TC6, TC7, TC8, and TC9. The cost is defined in (42) where k is the sample index from 1 to N, j reflects the jth index of thermocouple measurement available from the set of thermocouples $J = \{5,6,7,8,9\}$, and the hat signifies a quantity estimated by the model as opposed to a measured quantity, signified by no hat.

$$\text{cost} = \sum_{k=1}^{N} \left(\frac{\left| \hat{F}^{tp}_{NOx}(k) - F^{tp}_{NOx}(k) \right|}{\sum_{k=1}^{N} F^{fg}_{NOx}(k)} + \frac{\left| \hat{F}^{tp}_{HC}(k) - F^{tp}_{HC}(k) \right|}{\sum_{k=1}^{N} F^{fg}_{HC}(k)} + \frac{\sum_{j \in J} \left| \hat{T}_j(k) - T_j(k) \right|}{\sum_{j \in J} \sum_{k=1}^{N} 2000} \right) \tag{42}$$

The cost of (42) was minimized through iteration with the help of the gradient search routine "fminsearch" in MATLAB®[9]. In the process of model development, initially, data from simple tests was used to estimate coefficients and validate model changes. An example of such a test consists of operating the vehicle on a chassis dynamometer at a typical load corresponding to 15 MPH for the initial portion of the test, 30 MPH for the middle portion of the test, and 50 MPH for the final portion of the test. This results in feedgas levels of NOx and HC, and pattern of injected HC flow rate, as shown in Figure 5.

For the final "matured" version of the model, coefficients were optimized to Bags 1 and 2 of an FTP 75 test utilizing a pre-calibrated injection policy. The coefficients resulting from the fit are listed in Tables II, III, and IV. Plots of model inputs and outputs associated with this test are shown in Figures 6, 7, 8, and 9.

TABLE II
STORAGE MODEL COEFFICIENTS REGRESSED FROM DATA.

k_{in}	E_{in}	k_{out}	E_{out}	n_1	n_2	n_3	k_3	$k_{3'}$	E_3
600	891	0.380	873	0.334	2.60	0.667	50	88.4	795

[8]Typical real figures for cells per square inch are an order of magnitude larger, specifically 100-200 for a DPF and 200-400 for an ALNC.
[9]MATLAB is a registered trademark of The MathWorks, Inc.,Natick, MA.

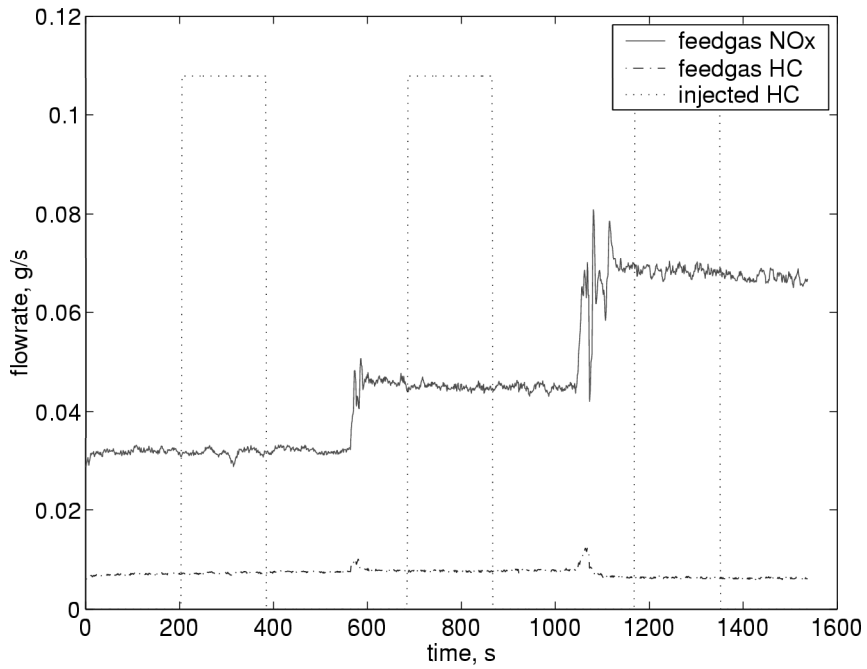

Fig. 5. Feedgas levels of NOx and HC, and injected HC, all in grams per second. Test set used for model fitting.

TABLE III
CHEMICAL MODEL COEFFICIENTS REGRESSED FROM DATA.

k_1	$k_{1'}$	E_1	k_2	E_2
8×10^6	1.6×10^7	289	4.5×10^4	428

TABLE IV
THERMAL MODEL CONVECTIVE COEFFICIENTS REGRESSED FROM DATA.

	Exhaust Section						
	1	2	3	4	5 & 6	7	8
h^i_{conv} $(W/(m^2K))$	0.607	12.6	0.200	13.7	0.001	2.49	0.068
h^o_{conv} $(W/(m^2K))$	6.08	77.9	0.001	0.001	11.3	29.0	9.18

C. Model Validation

To test the prediction capabilities of the model with the coefficients determined from the previous data set, the model was run on an independent data set shown in Figure 10. The results are shown in Figures 11, 12, and 13. The NOx and temperature predictions are good. It appears that the HC predictions are relatively off by a large factor. However, this error is very small when considered with respect to the feedgas levels of HC (as weighted in cost (42)). As a result, these errors would have a small impact on

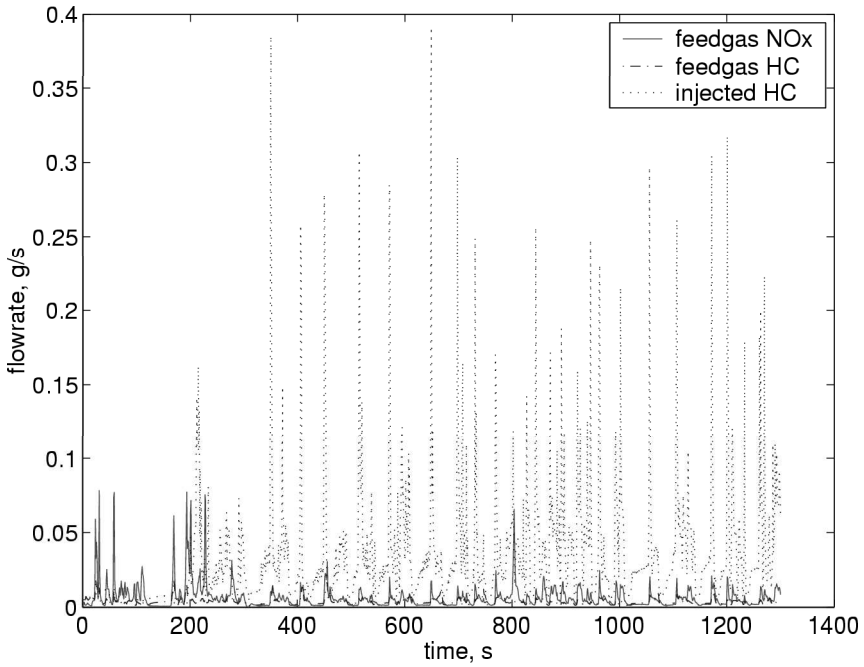

Fig. 6. Feedgas levels of NOx and HC, and injected HC, all in grams per second. Test set used for model fitting. (FTP 75 Bags 1 and 2 with calibrated injection)

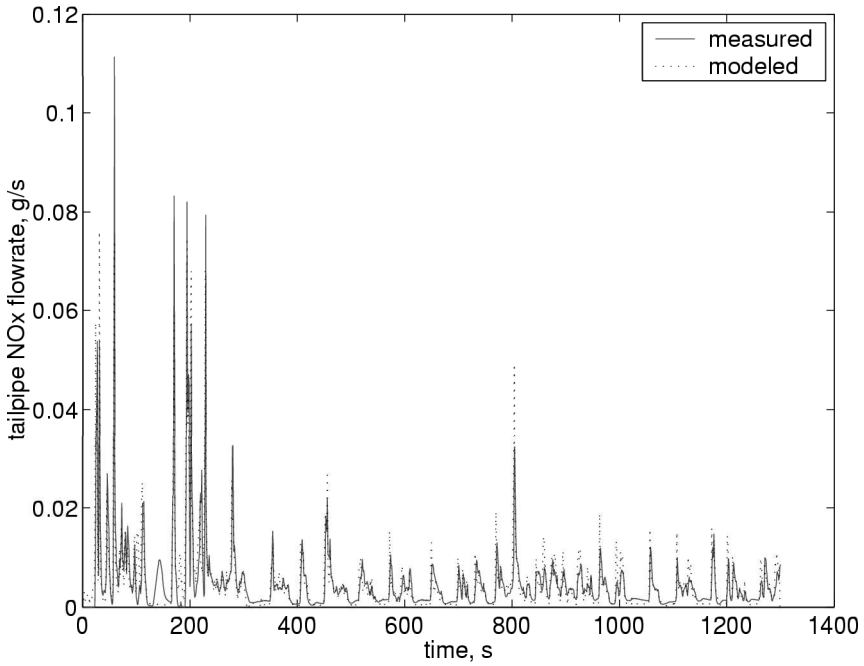

Fig. 7. Tailpipe NOx levels in grams per second. Test set used for model fitting. (FTP 75 Bags 1 and 2 with calibrated injection)

the NOx and thermal predictions and thus the model was accepted. Model emission conversion results for three independent FTP tests are summarized in Table V.

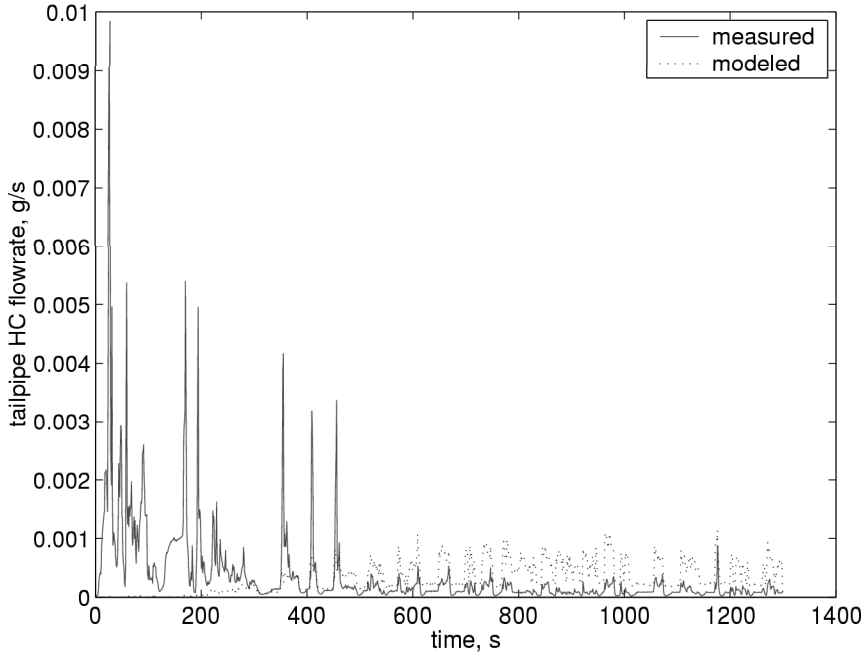

Fig. 8. Tailpipe HC levels in grams per second. Test set used for model fitting. (FTP 75 Bags 1 and 2 with calibrated injection)

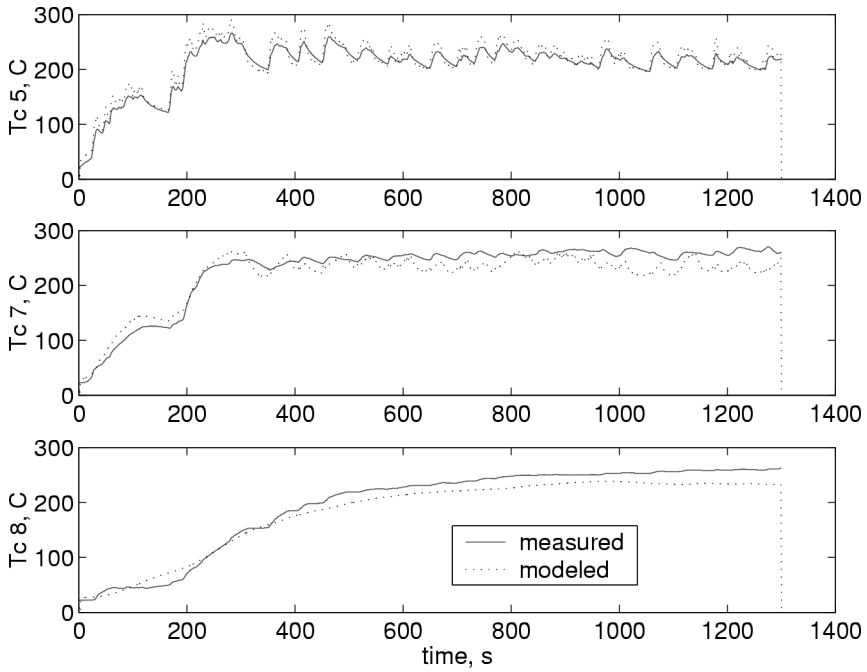

Fig. 9. Temperature comparisons for three thermocouple locations, in degrees Celsius. Test set used for model fitting. (FTP 75 Bags 1 and 2 with calibrated injection)

TABLE V
MODIFIED MODEL CONVERSION EFFICIENCY PREDICTION PERFORMANCE

Test (Bags 1 and 2 only)	Model Application	Measured Conversion		Modeled Conversion	
		NOx	HC	NOx	HC
FTP 75 : injection (Fig. 6 - 9)	fitting	26.9%	90.4%	26.7%	91.4%
FTP 75 : no injection (Fig. 10 - 13)	validation	11.3%	89.7%	9.0%	99.2%
FTP 74 : injection	validation	26.8%	94.7%	29.8%	92.6%

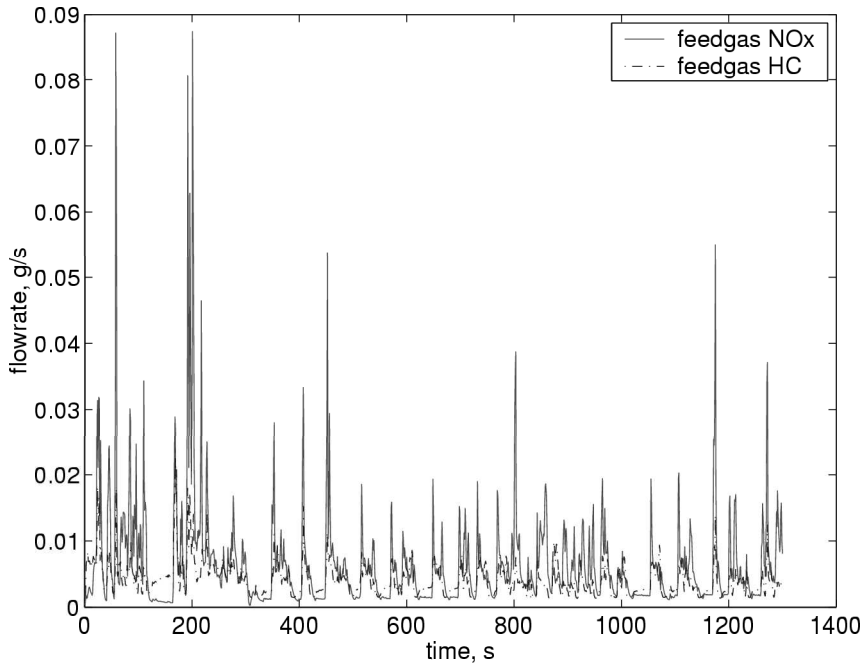

Fig. 10. Feedgas levels of NOx and HC, all in grams per second. Test set used for model validation. (FTP 75 Bags 1 and 2 with no injection)

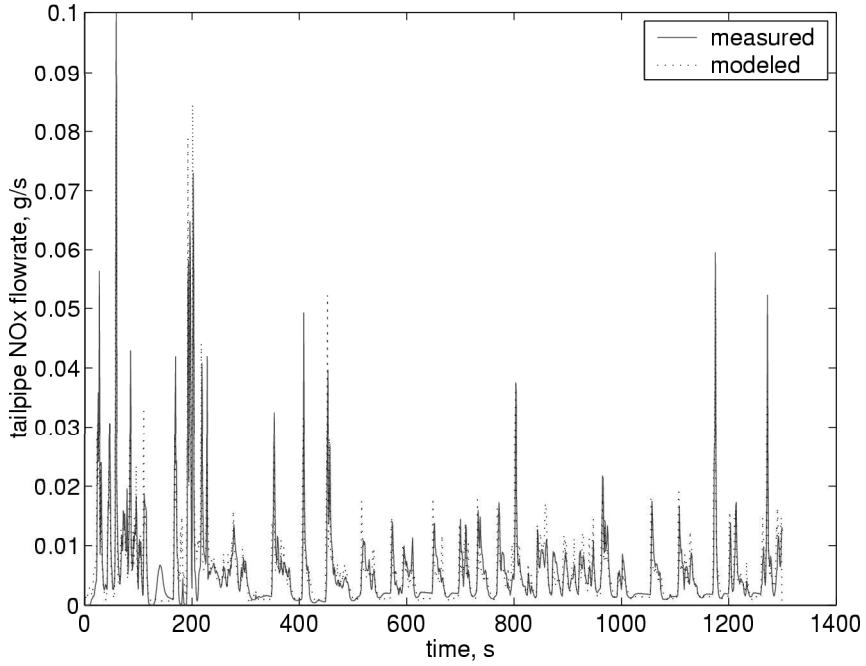

Fig. 11. Tailpipe NOx levels in grams per second. Test set used for model validation. (FTP 75 Bags 1 and 2 with no injection)

V. Model-Based Optimal Control Law Computation

The following section illustrates a control oriented application of the exhaust system model. Optimal control can be computed for a specified time trajectory of system inputs through the dynamic programming algorithm [2]. The resulting optimal control law is non-causal, however it can give motivation and insight

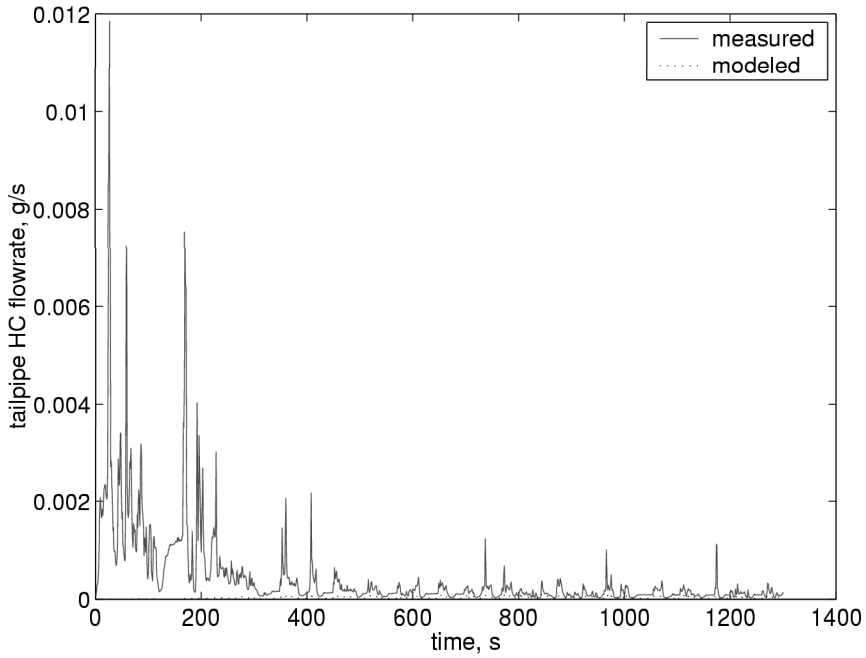

Fig. 12. Tailpipe HC levels in grams per second. Test set used for model validation. (FTP 75 Bags 1 and 2 with no injection)

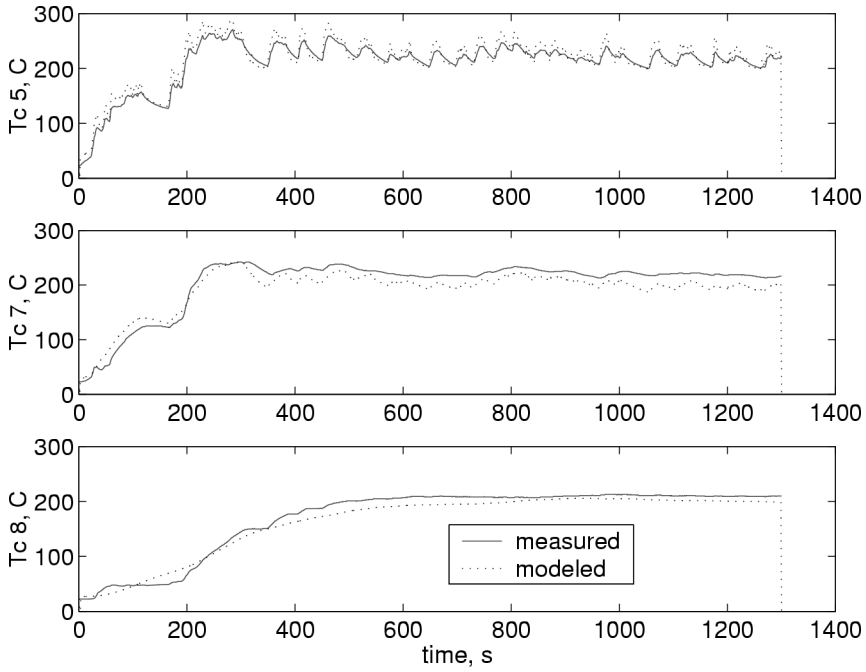

Fig. 13. Temperature comparisons for three thermocouple locations, in degrees Celsius. Test set used for model validation. (FTP 75 Bags 1 and 2 with no injection)

into potential for causal controller development. This is discussed more in detail in the following.

A. Optimal Control Law Computation Through Dynamic Programming - Problem Statement

This section formulates a finite horizon optimization problem for the diesel exhaust aftertreatment system. The model of the aftertreatment system, discretized for numerical optimization, can be expressed

as:

$$x(k+1) = f(x(k), u(k), \omega(k)) \tag{43}$$

$$y(k) = h(x(k), u(k), \omega(k)), \tag{44}$$

where $u(k)$ is the injected HC flow rate, $x(k)$ is the vector of states of the system, $\omega(k)$ is the vector of feedgas parameters, namely, exhaust flow rate, species concentrations, temperature and pressure, and $y(k)$ is the tailpipe NOx emissions flow rate. The objective of the optimization study is to evaluate the tradeoff in NOx emissions and fuel economy penalty [10]. The instantaneous cost is chosen as a weighted sum:

$$g(y(k), u(k), \omega(k)) = F_{NOx}^{tp}(k) + \mu F_{HC}^{inj}(k) = y(k) + \mu u(k). \tag{45}$$

For $\mu = 0$, the cost would reflect the desire to reduce tailpipe NOx emissions regardless of the amount of injected hydrocarbons required, whereas a sufficiently large value of μ would result in zero injected hydrocarbons.

In general, the emissions and fuel economy performance of a vehicle are evaluated through a specific drive test cycle such as the US FTP cycle, or the European Drive Cycle. Here, results are reported for Bags 1 and 2 of the US FTP 75 cycle on a warm start [11]. The objective is to find the optimal control sequence, $u(k)$, that minimizes the cost functional

$$J(x) = \min_{u \in U} \sum_{k=1}^{M} g(y(k), u(k), \omega(k)) = \min_{u \in U} \sum_{k=0}^{M} \bar{g}(x(k), u(k), \omega(k)), \tag{46}$$

where U represents constraints on u, such as a bound on flow rates, and M is the time length of the drive cycle. The cost (46) represents the cumulative weighted sum of tailpipe NOx emissions and injected hydrocarbons over the drive cycle. The objective will be to minimize the cost function, (46), for a range of μ. This will provide information on the sensitivity of tailpipe NOx emission levels to fuel economy penalty, and is more useful than just knowing the best NOx emission for a given upper bound on total injected hydrocarbons.

A systematic solution to the above problem can be determined recursively via Bellman's Dynamic Programming as described in [2]. Many practical aspects of the numerical solution of these equations are discussed in [5], and these techniques were adopted here.

[10] The injected hydrocarbons count against fuel consumption of the vehicle. Furthermore, tailpipe HC emissions is not considered as part of the cost since it is negligible for a lean environment when exhaust gas temperature is above T_{cut}.

[11] Specifically the first 1100 seconds of the FTP 75 Bags 1 and 2 cycle were used for controller development.

B. Model Reduction for Dynamic Programming

It is well-known and unfortunate that the computation time for solving the dynamic programming problem is exponential in the number of state variables and linear in the length of the time horizon. For this reason, a further simplification of the model was necessary in order to compute the optimal control. The model for the exhaust system identified earlier has a total of 18 states. In dynamic programming, with the computing technology at the time of this paper, beyond 2 or 3 states, the computational time quickly becomes impractical. Through a number of careful model reductions and a technique described as "State Aggregation" discussed in [1], this model was reduced to a 2 state model with reasonable replication of estimating capability as the full order model. The 2 states of the reduced order model were x_{HC}^{st1} and T_{p1}, or x_{HC}^{st} and T_p of the first ALNC [12]. Table VI shows how the reduced order model conversion efficiencies compared to the full order model and measured data.

TABLE VI
CONVERSION EFFICIENCY PREDICTION PERFORMANCE

Test (Bags 1 and 2 only)	Measured		Full Model		Reduced Model	
	NOx	HC	NOx	HC	NOx	HC
FTP 75 : injection	26.9%	90.4%	26.7%	91.4%	27.5%	91.5%
FTP 75 : no injection	11.3%	89.7%	9.0%	99.2%	9.7%	99.1%
FTP 74 : injection	26.8%	94.7%	29.8%	92.6%	29.9%	92.6%

In the following, the simplified model will be used to compute a family of optimal control laws. These control laws will then be evaluated on both the simplified model as well as the full model. It will be seen that the trends predicted by each are, to a large degree, quite similar. More will be said about this shortly.

C. Application of Dynamic Programming to the Reduced Model

The numerical dynamic programming solution methods of [5] were applied to the simplified, two state model to approximately compute the optimal policy. The states and controls were discretized as

$$\begin{aligned} x_{HC}^{st1} &\in \{0.1, 1.1, 2.1, \cdots, 16.1, 17.1, 18.1\} \times 10^{-2} \\ T_{p1} &\in \{300, 350, 400, 450, 465, 480, 495, 510, 525, 540, 600, 650, 750\} \\ F_{HC}^{inj} &\in \{0, 0.8, 1.6, 2.3, 3.1, 4.7, 7.0, 9.4, 11.7, 14.1, 16.4, 18.8, 21.1, 23.5\} \times 10^{-3}. \end{aligned} \tag{47}$$

The state discretization was chosen, after a small amount of trial and error, to cover the expected ranges of the model's state variables. The upper bound of 23.5×10^{-3} moles per second (or 325 milligrams per second) of injected fuel flow was quite arbitrarily selected as roughly an order of magnitude larger than

[12]Numerals appended to super/sub-scripts reflect the catalyst association. This notation will be followed from hereon.

the mean injection rates desired in this application [13]. Finally, the optimization problem was solved [14] for μ in the following set

$$\mu \in \{0, 0.25, 0.5, 1, 2, 4, 6, 8, 12, 16, 23, 64\} \times 10^{-3}. \tag{48}$$

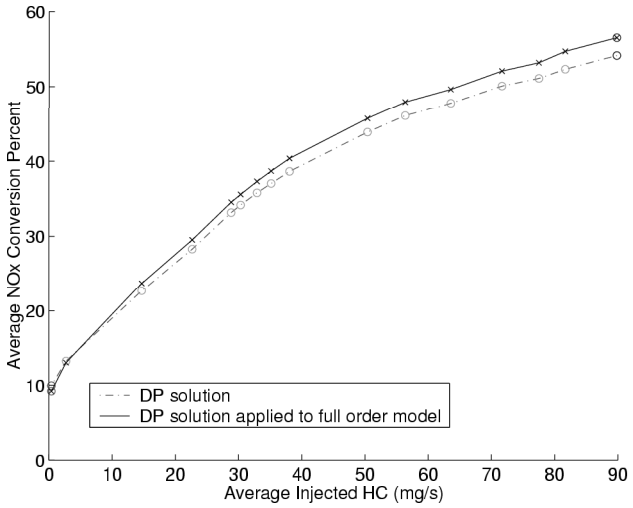

Fig. 14. Tradeoff curve for bags 1 and 2 of the FTP cycle: NOx conversion efficiency versus average injected HC rate as determined by dynamic programming applied to the simplified model and the complete model.

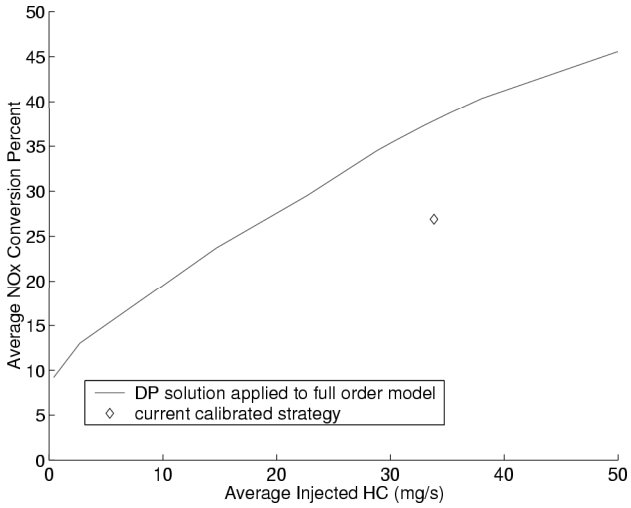

Fig. 15. The calibrated injection strategy plotted relative to the tradeoff curve for bags 1 and 2 of the FTP cycle, determined by the dynamic programming solution applied to the complete model, shown for 0 to 50 mg/s average injection.

The resulting tradeoff curve for the simplified model is shown as the dotted line in Figure 14; the optimal injection policy determined on the basis of the simplified model was also *evaluated* [15] on the complete model, resulting in the solid tradeoff curve in the same figure. In Figure 14, the simplified model and complete model simulation capture similar trends in that both recognize the initial rapid and later shallow increase of NOx conversion with increasing average injected HC flow rate. The optimal policy of the simplified model is sub-optimal for the full model. Though the results between the simplified model and complete model differ by up to almost 5% absolute NOx conversion at the higher end of the average injection range of 0 to 90 mg/s, these portions of higher HC injection rate are not relevant for controller design. Because of fuel economy reasons, the injection penalty range of interest was chosen between roughly 20 and 45 mg/s. Figure 15 shows the full order model curve plotted for injection rates between 0 and 50 mg/s along with an experimental data point.

In parallel with the analytical work reported here, a controller for the aftertreatment system was developed as a part of on-vehicle calibration. The controller relied on quantities easily measured on

[13]Increasing upper bound of injection milligrams per second does not appreciably alter the results.

[14]The optimal dynamic programming solution is in the form $u_\mu(x_0, k)$ where x_0 denotes the initial state vector. For all dynamic programming optimization solutions, an initial state vector of $x_{HC}^{st1} = 2.1 \times 10^{-2} mol$ and $T_{p1} = 300K$ (ambient) was used to reduce the solution to $u_\mu(k)$. The storage state corresponds to the final storage resulting from simulation of a FTP 75 cycle Bags 1 and 2 without injection beginning from zero initial storage. Warm or cold start yields similar final storage amount.

[15]The optimization was not performed on the full model.

the diesel engine in order to determine when and how much HC to inject in the exhaust system. This controller injects roughly 35 mg/s average over FTP 75 Bags 1 and 2 and achieves a NOx conversion efficiency of 27% [16]. It is plotted relative to the tradeoff curve in Figure 15.

VI. Conclusions

This work has developed a control-oriented phenomenological model of an active lean NOx catalyst (ALNC). The model consists of three key parts: HC storage, NOx reduction, and heat transfer through the catalyst body between the exhaust gas and ambient air. In addition, a heat transfer model was provided for the exhaust pipes and diesel particulate filter (DPF). The individual models were assembled into an overall model of an exhaust aftertreatment system. Model parameters were estimated through regression against experimental data.

To illustrate use of the model, dynamic programming was employed to determine the optimal HC injection policy over a drive cycle. Such studies can be very useful for system prototyping and component sizing. A causal approximation of the non-causal optimal policy was implemented on a vehicle. It compared well with another controller developed as part of on-vehicle calibration.

Acknowledgments

J.W. Grizzle gratefully acknowledges funding under Ford Motor Company URP 2000-212R, *Active Control of Aftertreatment for Improved Emissions and Fuel Economy*. D. Aswani gratefully acknowledges a Ford Summer-2001 Internship.

References

[1] J. C. Bean, J. R. Birge, R. L. Smith, "Aggregation in Dynamic Programming," Operations Research, Vol. 35, No. 2, March-April 1987.
[2] Dimitri P. Bertsekas, *Dynamic Programming and Optimal Control*, Athena Scientific, 1995.
[3] C. Havenith, P. Verbeek, D. Heaton and P. van Sloten, "Development of a Urea DeNOx Catalyst Concept for European Ultra-Low Emission Heavy-Duty Diesel Engines," SAE paper 952652, Detroit.
[4] J. B. Heywood, *Internal Combustion Engine Fundamentals*, McGraw-Hill, NY, 1988.
[5] J.-M. Kang, I. Kolmanovsky and J. W. Grizzle, "Dynamic Optimization of Lean Burn Engine Aftertreatment," to appear in *ASME J. Dynamic Systems Measurement and Controls*.
[6] H. Klein, S. Lopp, E. Lox, M. Kawanami and M. Horiuchi, "Hydrocarbon DeNOx catalysis-System Development for Diesel Passenger Cars and Trucks," SAE paper 1999-01-0109, Detroit.
[7] P. Laing, M. Shane, S. Son, A. Adamczyk, and P. Li, "A Simplified Approach to Modeling Exhaust System Emissions: SIMTWC," SAE paper 1999-01-3476, Detroit.
[8] J. Leyrer, E.S. Lox and W. Strehlau, "Design Aspects of Lean Nox Catalysts for Gasoline and Diesel Applications," SAE paper 952495, Detroit.
[9] J. Leyrer, E. S. Lox, K. Ostgathe, W. Strehlau, T. Kreuzer, G. Garr "Advanced Studies on Diesel Aftertreatment Catalysts for Passenger Cars," SAE paper 960133, Detroit.
[10] H. Lüders, P. Stommel and S. Geckler, "Diesel Exhaust Treatment- New Approaches to Ultra Low Emission Diesel Vehicles," SAE paper 1999-01-0108, Detroit.
[11] A. Peters, H.-J. Langer, B. Jokl, W. Müeller, H. Klein and K. Ostgathe, "Catalytic NOx reduction on a Passenger Car Diesel Common Rail Engine," SAE paper 980191, Detroit.
[12] R. Sonntag and C. Borgnakke, *Introduction to Engineering Thermodynamics*, John Wiley and Sons, Inc. New York, 2001.
[13] M. van Nieuwstadt, "Modeling and Dynamic Control of an Active Lean NOx Catalyst," *American Control Conference*, June 2001, Arlington.
[14] Y. Wang, S. Raman and J. Grizzle, "Dynamic Modeling of a Lean NOx trap for Lean Burn Engine Control," ACC 1999, San Diego.

[16] An average injection rate of 30-40 mg/s for the FTP 75 cycle was provided as a target corresponding to less than 1 mpg penalty in fuel economy for the vehicle under study